

THE INJECTION CHICANE OF THE NBS-LOS ALAMOS RACETRACK MICROTRON

P.H. Debenham, S.S. Bruce, S. Penner, and M.A.D. Wilson*
National Bureau of Standards, Gaithersburg, MD 20899

Abstract

Injection of 5 MeV electrons into the NBS-Los Alamos racetrack microtron is accomplished with a dipole magnet on the linac axis. A three-magnet chicane is used to compensate for the unwanted deflection of recirculating beam by the injection magnet. In order to minimize emittance growth due to power supply noise, the three chicane magnets are driven by two power supplies, with each supply connected in series to two coils in different magnets. This arrangement, together with the tight space available for the chicane, constrains the choice of conductors, and leads to very precise and compact low-field magnets. Magnetic field measurements demonstrate that all design goals have been achieved.

Introduction

Injection of 5 MeV electrons into the NBS-Los Alamos racetrack microtron (RTM)¹ is accomplished by deflecting the beam from the injector by 15 degrees into the RTM linac. In Figure 1, D6 is the dipole magnet used for injection. The 5 MeV beam is then accelerated to 17 MeV by the linac and deflected through 180 degrees by end magnet E1 to re-enter the linac at the other end. Dipole magnets D7 and D8 compensate for the displacement of the 17 MeV beam by E1 so that it re-enters the linac on axis.² The 17 MeV beam is then accelerated to 29 MeV in the opposite direction by the (standing-wave) linac.

The 29 MeV beam encounters the injection chicane, which comprises magnets D6, D9, and D10. It is then deflected through 180 degrees by end magnet E2, bypasses the linac in a return line, and is returned to the linac by magnets E1, D8, and D7 for further acceleration. Magnets D8 and D7 give an unwanted parallel dis-

placement, Δx , to the beam at 29 MeV and above. Uncorrected, this displacement would cause the beam to re-enter the linac off axis. At 29 MeV, $\Delta x = 2.4$ cm. Dipole magnets D9 and D10 in the chicane compensate for this effect by displacing the beam by $-\Delta x$ before it encounters magnets D8 and D7. In addition, magnet D9 compensates for the unwanted deflection of recirculating beam by magnet D6, a deflection of three degrees at 29 MeV.

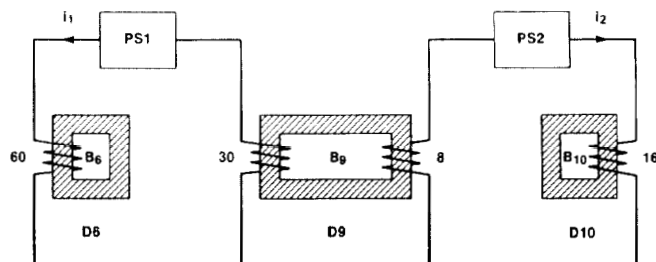


FIG. 2. Configuration of chicane magnet coils and power supplies. The number of turns per coil is given.

Magnet and Power Supply Configuration

The three chicane magnets are driven by two power supplies, as shown in Figure 2. The air gaps of all three magnets are equal. The effective lengths of magnets D6 and D10 are equal, and are half that of magnet D9. Power supply 1 drives current i_1 through the coil of magnet D6, then, in the opposite direction, through a coil in magnet D9. The D9 coil has half as many turns as the D6 coil, so the magnetic field in D9 produced by i_1 is half of, and antiparallel to, that in D6. The angular deflection of a beam in a magnet is

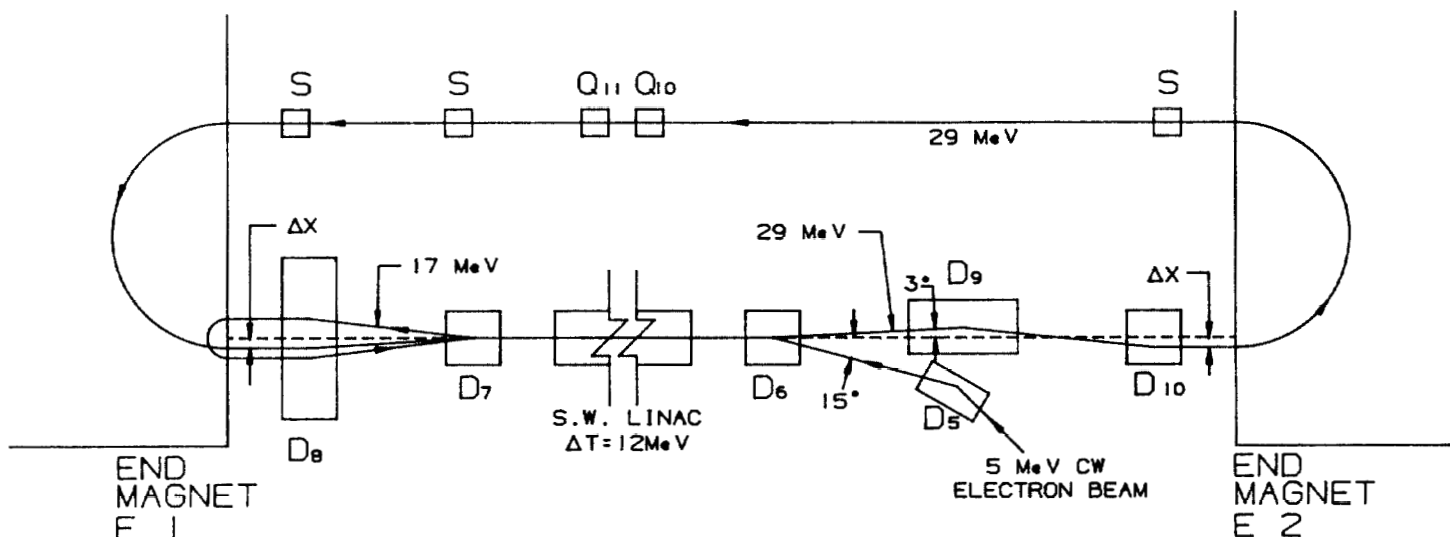


FIG. 1. Injection and first two recirculating orbits in the NBS-Los Alamos RTM. Higher-numbered orbits, which are omitted for clarity, are similar to the 29 MeV orbit but with bend radii in the two end magnets that increase with energy. D designates a dipole magnet, Q a quadrupole magnet, and S a steering magnet. Not to scale.

*Supported in part by the Division of Nuclear Physics, US DoE

proportional to the magnetic field integrated over the pathlength, or "field integral". The field integrals for magnets D6 and D9 due to power supply 1 are equal in magnitude but opposite in sign. Therefore, the net field integral due to power supply 1 is very nearly zero. Consequently, power supply 1 imparts a parallel displacement to the beam, with little angular deflection. Similarly, power supply 2 drives current i_2 through a second coil in magnet D9 in series with the coil in magnet D10, and produces equal and opposite magnetic field integrals in magnets D9 and D10.

The chicane configuration was chosen for several reasons. First, each power supply controls one of the two desired functions of the chicane. Power supply 1 is set to deflect the 5 MeV beam onto the linac axis with magnet D6; power supply 2 is adjusted to give the desired parallel displacement $-\Delta x$ to the 29 MeV beam with magnets D9 and D10. Second, each power supply produces a parallel displacement of the beam with very little angular deflection. This is essential to minimizing the contribution of magnet power supply noise to emittance growth, especially since the beam makes as many as 14 passes through the chicane. The criterion for negligible emittance growth for a magnet on the linac axis is that the product of the net field integral produced by the power supply and the percent current regulation of the power supply should not exceed $3 \text{ G}\cdot\text{cm}\cdot\%$. This was achieved for both chicane power supplies by designing the magnets carefully to match the field integrals produced by series-connected coils, and by using power supplies having 10^{-4} regulation.

Ideally, the chicane as a whole would produce a pure parallel displacement of the beam. In reality, it also produces some small angular deflection, but this can be compensated with steering magnets on the return beam lines. Negligible emittance growth from the available 10^{-3} regulated steering magnet power supplies is ensured if the chicane field integral is less than $125 \text{ G}\cdot\text{cm}$. The measured value is $58 \text{ G}\cdot\text{cm}$.

Magnet Design and Performance

Two-dimensional magnet field calculations were performed using TRIM³ to design the chicane magnets for the desired magnetic field integrals and field uniformity. To limit emittance growth to an acceptable level, the relative sextupole component, ϵ , of RTM dipole magnets must be $7 \times 10^{-4} \text{ cm}^{-2}$ or less. The chicane magnets were fabricated of AISI 1006 carbon steel to achieve this degree of field uniformity. Field clamps, shown in Figure 3, are used to control the effective length of the magnets. The magnets were field-mapped with a Hall-probe apparatus that is described in reference 2. All design goals were achieved. Measured properties of the magnets are given in Table 1.

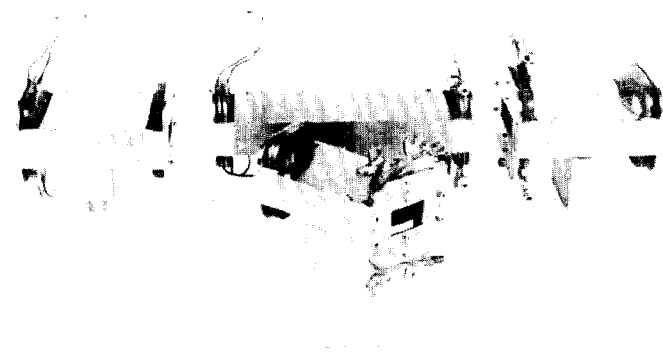


FIG. 3. Chicane magnets, with magnet D5 in foreground. In back are D6, D9, and D10, from left to right.

TABLE 1. Measured properties of the chicane magnets. L is the effective length, N and I are the number of turns and current in the coil, and ϵ is the relative sextupole field coefficient.

Magnet	Gap (cm)	L (cm)	NI (A)	B_0 (G)	$B_0 \cdot L$ (G·cm)	ϵ (cm^{-2})
D6	2.59	12.60	788.9	380.0	4789	3×10^{-4}
D9	2.59	25.06	1369.0	-661.8	-16,585	2×10^{-4}
D10	2.59	12.56	1949.2	943.8	11,585	5×10^{-5}

The width of magnet D9 is limited by its proximity to magnet D5 in the injection transport line, as shown in Figure 1. To minimize the width, a picture-frame design is used, and one coil is made of hollow, water-cooled conductor, as shown in Figure 4. In order to limit the number of high-current power supplies, the other coil (the one in series with D6) is made of solid conductor. The solid coil is cooled by conduction to the water-cooled coil, and is located inside it to permit a workable lead configuration. The side yoke is as thin as possible without the internal magnetic field exceeding 10 kG. The top and bottom yoke thickness was chosen for good field uniformity in design calculations. Calculated and experimental transverse field profiles for magnet D9 are given in Figure 5.

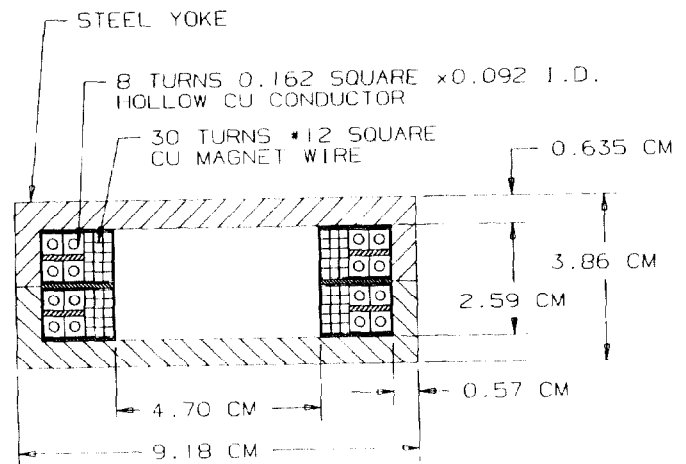


FIG. 4. Cross section of magnet D9.

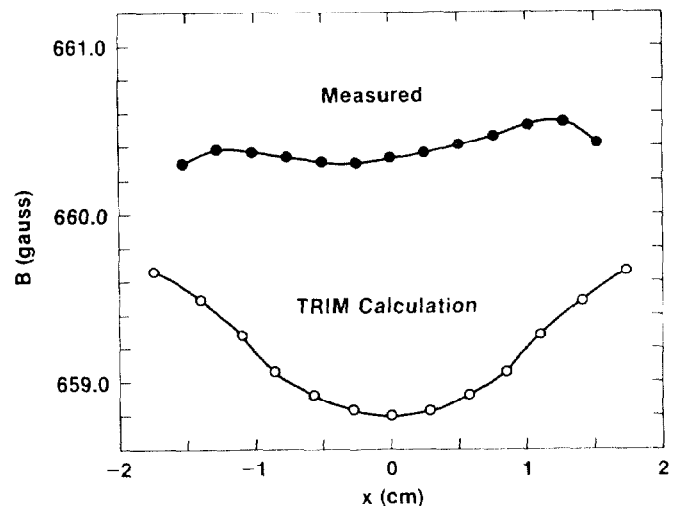


FIG. 5. Magnetic field B in magnet D9 versus x, the transverse distance from the magnet axis in the plane of bending.

Magnet D6, shown in Figure 6, is a picture-frame magnet with the same gap dimension as D9. It contains a solid-conductor coil that is powered in series with the solid coil in D9. Cooled by convection only, the D6 coil is made of larger wire to reduce the power density and limit the operational temperature rise to 30°C. The D6 coil must contain 60 turns to match the field integral produced by the D9 coil in series. Because the wire is larger in D6, ten layers do not fit in the gap, as in D9. Instead, eight layers of seven turns are used, plus four extra turns. The extra turns are located at the outside of the coil to minimize their effect on the beam. They are located symmetrically in the middle of the half-gaps, the position for which design calculations predicted the best field uniformity. The top and bottom yokes are thicker than in the other magnets to offset the reduced permeability at the lower field of D6. Calculated and experimental transverse field profiles for magnet D6 are given in Figure 7.

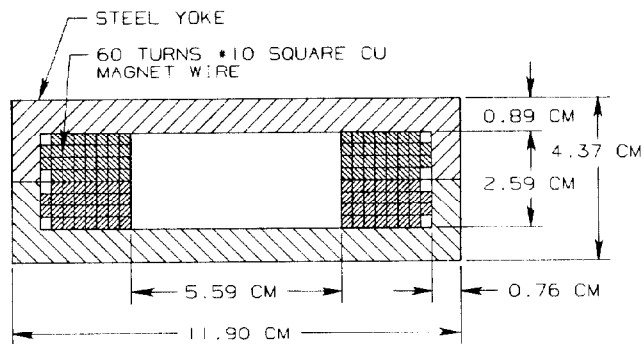


FIG. 6. Cross section of magnet D6.

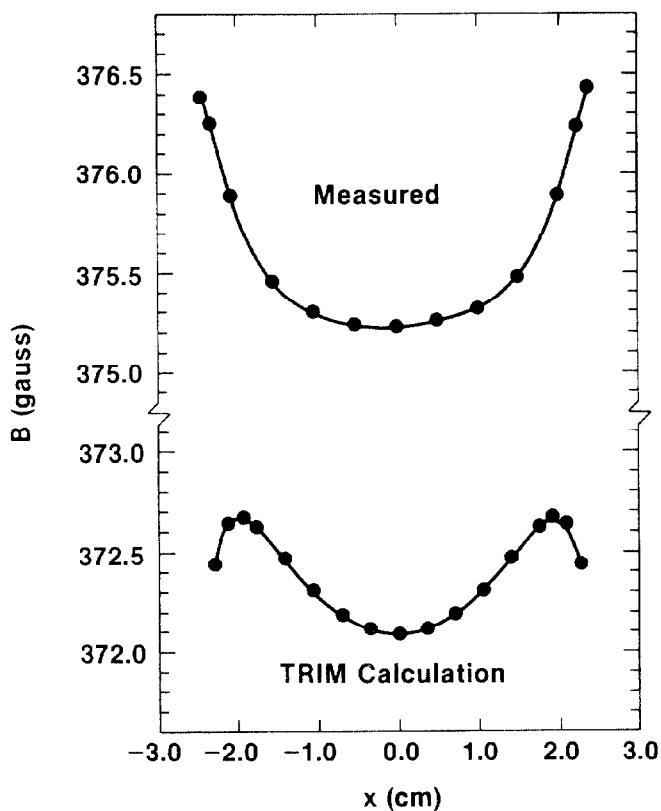


FIG. 7. Magnetic field B in magnet D6 versus x.

Magnet D10, shown in Figure 8, is a picture-frame magnet with the same gap dimension as D9. Its hollow-conductor coil has twice the number of turns as the hollow-conductor coil in D9 and is powered in series with it. Calculated and experimental transverse field profiles for magnet D10 are given in Figure 9.

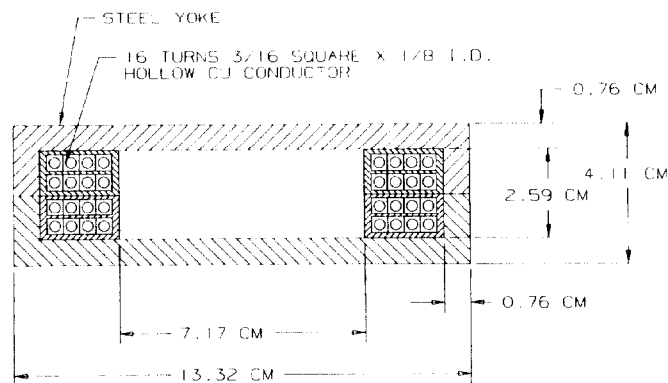


FIG. 8. Cross section of magnet D10.

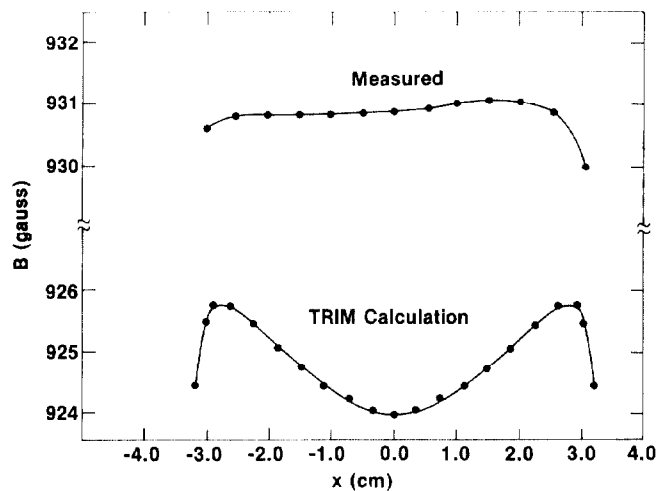


FIG. 9. Magnetic field B in magnet D10 versus x.

References

1. S. Penner et al., IEEE Trans. Nucl. Sci. **NS-32** (1985) 2669.
2. M. Wilson et al., "Orbit-reversing magnets for the NBS-Los Alamos racetrack microtron," proceedings of this conference.
3. A. M. Winslow, J. Comput. Phys. **1** (1966) 149.